Almost-Uniform Sampling of Rotations for Conformational Searches in Robotics and Structural Biology

Yan Yan and Gregory S. Chirikjian

Abstract— We propose a new method for sampling the rotation group that involves decomposing it into identical Voronoi cells centered on rotational symmetry operations of the Platonic solids. Within each cell, Cartesian grids in exponential coordinates are used to achieve almost-uniform sampling at any level of resolution, without having to store large numbers of co-ordinates, and without requiring sophisticated data structures. We analyze the shape of these cells, and explain how this new method can be used in the context of conformational searches in the fields of Robotics and Structural Biology.

I. INTRODUCTION

In many application areas ranging from robot motion planning to computational structural biology, the issue of how to uniformly sample rotations arises. Moreover, the problem of sampling uniformly at random is a very different problem than constructing schemes to uniformly sample deterministically. The former can be achieved by using the standard inverse-function technique in, for example, the Euler angle parameterization, or by using one of the many other techniques described in [1], [2], [3]. Random uniform sampling on the rotation group, $SO(3)$, is much easier than deterministic uniform sampling, the latter of which does not even have an exact solution (except for the very coarse samplings corresponding to the rotational symmetry operations of the Platonic solids). This is because random sampling only depends on the Jacobian determinant, $|J(\mathbf{q})|$, when a particular parameterization of rotation matrices, $R(\mathbf{q})$, is used. In contrast, a measure of equal spacing depends on the invariant distance metric that is used. A distortion measure then can be constructed that measures how different the metric tensor is from the identity matrix as

$$C(\mathbf{q}) = \frac{1}{\sqrt{3}} \|G(\mathbf{q}) - \mathbb{I}\|. \tag{1}$$

Here $G(\mathbf{q}) = J^T(\mathbf{q})J(\mathbf{q})$, $\|\cdot\|$ denotes the Frobenious norm, and $\sqrt{3} = \|\mathbb{I}\|$ is used as a normalizing factor. It is known that it is not possible to construct perfectly uniform finely spaced samples in the sense of having $C(\mathbf{q}) = 0$ for all possible values of $\mathbf{q}$ for $R(\mathbf{q})$ to densely fill $SO(3)$. The next natural question to then ask is "how good of a fine sampling of $SO(3)$ is achievable ?"

The issue of "as uniform as possible" sampling on $SO(3)$ is very closely related to the analogous problem on the sphere. Several related problems have been studied in very different bodies of literature. On the one hand, spherical designs and spherical codes [4], [5], [6], [7] seek to place

The authors are with the Department of Mechanical Engineering, Johns Hopkins University, Baltimore, MD 21218, USA `gregc@jhu.edu`

points on the sphere in order that the distance between nearest neighbors is as uniform as possible. This is related to, but not exactly the same as, the problem of packing equal sized circles on the surface of the sphere as described in [8], [9], [10], [11]. So-called "cubature" rules [12], [13] seek to define points on the surface of the sphere so as to sample bandlimited spherical harmonic expansions and turn integrals into discrete sums (as in quadrature rules).

The issue of how to uniformly sample the rotation group, $SO(3)$, which also goes by different names in other fields (such as the "orientational space," "Eulerian space", etc.) has received attention in various fields from robotics and computer graphics to problems in crystallography and biomolecular structure determination. In many cases, variants of the ZXZ or ZYX Euler angles $\mathbf{q} = [\alpha, \beta, \gamma]^T$ are used in which, for example, the two Z rotations are sampled uniformly and the middle Euler angle is sampled according to a $\beta = \cos^{-1}(x)$ rule where x is sampled uniformly from $[-1, 1]$. In this way equal volume partitions of $SO(3)$ are achieved, since the integration measure for $SO(3)$ in these parameterizations has a $\sin\beta$ factor, much like the unit sphere S^2. But equal volume partition (as studied in [14]) is not the same as equal spacing of sample points. For example, cells that are box-like regions can be long and narrow or close to cubical and still have the same volume, but the vertices of the cells in the former case would not be uniformly distributed. Therefore, placing constraints on equal volume cells is not the same as placing constraints on equal shape cells. And even having cells of equal shape does not imply that points on the vertices of these cells are uniformly spaced.

The Euler angles are particularly bad when it comes to uniform sampling as measured by (11). A variant on the Euler angles is the so-called Lattman angles [15]. These angles are defined relative to the Euler angles as $(\phi, \theta, \psi) = (\alpha + \gamma, \beta, \alpha - \gamma)$. This means that $G(\phi, \theta, \psi)$ will at least be diagonal in the computation of the cost function in (11), and thereby cancel with more of the identity matrix than $G(\alpha, \beta, \gamma)$, which is not even diagonal.

More recently, a number of papers have addressed how to generate close-to-uniform samplings on the sphere, torus, rotation group, and other manifolds by minimizing various energy functions [16], [17], recursive subdivisions [18], [19], interpolation using distance metrics [20], [21], quadrature-based methods [22], [23], and a fibration approach [24], [25].

These approaches all have merit, but in some cases require sophisticated recursion schemes or storing coordinates. We take a very different group-theoretic approach rather than the geometric approaches discussed above. Namely, we partition

the rotation group into Voronoi cells, where the distance metric used is one of those reviewed in [26], and the center points of each cell is an element of one of the rotational symmetry groups of the platonic solids. Then, in the Voronoi cell centered on the identity, we construct a Cartesian grid in exponential coordinates. Because the exponential parameterization is almost linear near the identity, the distortion measure is close to zero. The contents of the Voronoi cell near the identity are then replicated in the other cells by left-shifting the contents by each rotational-symmetry operation corresponding to the symmetry group used to construct the cells. We study the shapes of these cells for the tetrahedral, octahedral, and icosahedral groups. The icosahedral case is particularly interesting because $SO(3)$ is divided into 60 small identical units, and the distortion in the exponential parameterization is very small over each one. This means that rotations can be sampled very simply on a Cartesian grid in the Lie algebra and exponentiated.

II. OUR METHOD OF SAMPLING ON $SO(3)$

A. Parameterization $SO(3)$ as a Solid Ball in $\mathbb{R}^3$ in Exponential coordinates

The rotation group $SO(3)$, i.e., the special orthogonal group, is the set of all rotations about the origin of three-dimensional Euclidean space $\mathbb{R}^3$ together with the operation of composition. By definition, a rotation about the origin is a linear transformation that preserves length of vectors, angles between vectors, and handedness of space. The elements of $SO(3)$ can be represented as 3×3 orthogonal matrices with unit determinant, in which case the group operation becomes matrix multiplication. Different coordinates can be used to parametrize $SO(3)$. The commonly used ones are axis-angle representation (also known as exponential coordinates), Euler angles, hyper-spherical coordinates, quaternions and etc..

In this paper, we parameterize $SO(3)$ as a solid ball in $\mathbb{R}^3$ with radius π in exponential coordinates [27]. In this description, the radius of each concentric spherical shell within the ball represents a rotation angle. With a unit vector $\mathbf{n}$ indicating the rotation axis and an angle θ describing the amount of rotation around $\mathbf{n}$, any rotation matrix $R \in SO(3)$ can be represented as

$$R = \exp(\hat{\mathbf{n}}\theta) = \mathbb{I} + \hat{\mathbf{n}}\sin\theta + \hat{\mathbf{n}}^2(1 - \cos\theta), \qquad (2)$$

where

$$\hat{\mathbf{n}} = \begin{pmatrix} 0 & -n_3 & n_2 \\ n_3 & 0 & -n_1 \\ -n_2 & n_1 & 0 \end{pmatrix}$$

is the skew-symmetric matrix corresponding to $\mathbf{n}$. This can be viewed as spherical coordinates in the Lie algebra $so(3) \cong \mathbb{R}^3$ in which θ takes the place of the radius. The corresponding Cartesian coordinates are $\mathbf{x} = \theta\mathbf{n}$ where $\theta = \|\mathbf{x}\|$ and $\mathbf{n} = \mathbf{x}/\|\mathbf{x}\|$. In component form,

$$\mathbf{x}(\theta,\alpha',\beta') = \theta \begin{pmatrix} \sin\alpha'\cos\beta' \\ \sin\alpha'\sin\beta' \\ \cos\alpha' \end{pmatrix} = \begin{pmatrix} x \\ y \\ z \end{pmatrix} = \begin{pmatrix} n_1\theta \\ n_2\theta \\ n_3\theta \end{pmatrix},$$
$$(3)$$

where $-\pi \leq \theta \leq \pi$, $0 \leq \alpha' \leq \pi$, $0 \leq \beta' \leq 2\pi$ and $\mathbf{x} = [x, y, z]^T$ are the Cartesian coordinates for the points inside the ball. We can obtain the same rotation matrix in (2) by exponentiating the skew-symmetric matrix corresponding to $\mathbf{x}(\theta,\alpha',\beta')$. (Here we use α' and β' to distinguish from the first two Euler angles α and β mentioned earlier).

B. Discrete subgroups of $SO(3)$

A subset $H \in G$ is said to be a discrete subgroup of G if it contains only isolated elements of G and is closed under the group operation. Three discrete subgroups of the rotation group $SO(3)$ correspond to symmetry operations of the Platonic solids —the tetrahedral group T, the octahedral group O, and the icosahedral group I. Another family of discrete subgroups of $SO(3)$ are the cyclic groups C_n which result from sampling rotations around a fixed axis at angles of $2\pi/n$. The rotational symmetry groups of the platonic solids can be described in terms of cyclic groups of different orders applied to their faces, edges, and vertices so as to leave the volume occupied by the solids unchanged.

A regular tetrahedron has four $4\, C_3$ axes through each vertex to the center of the opposite face, and $3\, C_2$ axes through the centers of pairs of opposite edges. Including the identity, the total number of group elements of T is $4(3-1)+3(2-1)+1 = 12$. The cube and its dual, the octahedron, have $3\, C_4$ axes through the centers of opposite faces, $4\, C_3$ axes through opposite vertices, and $6\, C_2$ axes through the centers of pairs of opposite edges. The total number of group elements of O is $3(4-1)+4(3-1)+6(2-1)+1 = 24$. The icosahedron and its dual dodecahedron have $6\, C_5$ axes through opposite vertices, $10\, C_3$ through the centers of opposite faces, and $15\, C_2$ axes through the centers of opposite edges. Thus, the subgroup I has $6(5-1)+10(3-1)+15(2-1)+1 = 60$ elements.

C. Generating Voronoi Cells of $SO(3)$

In this paper, we decompose $SO(3)$ into Voronoi cells centered on elements of its discrete subgroup Γ (Γ can be T, O or I), with each Voronoi cell consisting of the points contained in $SO(3)$ closer to one element of Γ than to any other. A common metric to define the distance between any two points $R_1, R_2 \in SO(3)$ is

$$d(R_1, R_2) = \theta(R_1^T R_2) = \|(\log(R_1^T R_2))^\vee\| \qquad (4)$$

where $\log(\cdot)$ is the inverse of the exponential mapping in (2), which is valid when $\theta \in [0, \pi)$. This is extended to the closed solid ball by simply setting $\theta(R_1^T R_2) = \pi$ on the boundary. Here, as earlier, $\|\cdot\|$ is the Euclidean norm, and $\vee$ is defined by the property that $(\hat{\mathbf{x}})^\vee = \mathbf{x}$.

The Voronoi cells of $SO(3)$ represented in the exponential coordinates can partition the solid ball in $\mathbb{R}^3$ into separate regions, denoted as $S_1, S_2, \cdots, S_m$, where m is the number of elements in Γ (see Fig. 1 for the octahedral group). These regions are mildly ambiguous at their borders, but this represents a set of measure zero. The region S_1 located in the center of the solid ball corresponds to the Voronoi cell of the identity matrix. Because the exponential parameterization

is relatively flat near the identity, i.e., $\exp \hat{\mathbf{x}} \approx \mathbb{I} + \hat{\mathbf{x}}$ when $\|\mathbf{x}\| << 1$, the metric tensor becomes $G(\mathbf{x}) \approx \mathbb{I}$, and the distortion measure $C(\mathbf{x})$ of the samples on $SO(3)$ parametrized by Cartesian grids on the S_1 is close to zero. And the smaller size of S_1, the smaller the overall distortion will be. Subsequently, the samples of other Voronoi cells of $SO(3)$ can be obtained from the samples computed for the "center" Voronoi cell (i.e., the one that corresponds to the identity element of $SO(3)$ and Γ) by multiplying with the other rotation matrices in Γ. In other words, after we generate N samples for the center Voronoi cell, for every other Voronoi cell $S_k \subset SO(3)$, we replicate the N samples by shifting those from the center cell, S_1. This can be done by either left or right shift:

$$\{\exp(\hat{\mathbf{x}}_{k_i})|i = 1, \cdots, N\} = \{\exp(\hat{\mathbf{x}}_{1_i})R_k|i = 1, \cdots, N\} \quad (5)$$

or

$$\{\exp(\hat{\mathbf{x}}'_{k_i})|i = 1, \cdots, N\} = \{R_k \exp(\hat{\mathbf{x}}_{1_i})|i = 1, \cdots, N\}, \quad (6)$$

for all $k = 2, \cdots m$ where $\{\hat{\mathbf{x}}_{k_i}|i = 1, \cdots, N\}$ and $\{\hat{\mathbf{x}}'_{k_i}|i = 1, \cdots, N\}$ are the N samples for the center Voronoi cell generated by these shifts, and R_k is the element of the discrete subgroup Γ. Note that while in general at the level of individual samples $\mathbf{x}_{k_i} \neq \mathbf{x}'_{k_i}$, at the level of whole cells

$$\overline{S_k} = R_k \cdot \overline{S_1} = \overline{S_1} \cdot R_k$$

where $\overline{S_k}$ denotes the closure of cell S_k and $\cdot$ denotes the application of R_k to each point in $\overline{S_k}$.

Thus, without loss of generality, we can focus on sampling the center Voronoi cell, and samples of the rest of $SO(3)$ can be obtained by shifting the samples from the center one, without introducing more distortion. The reason why we can shift from either the left or the right is that the metric in (4) used to generate the Voronoi cells is left and right invariant, i.e., $d(R_1, R_2) = d(AR_1, AR_2) = d(R_1A, R_2A)$ for any $A \in SO(3)$. Therefore, the Voronoi cells that we are considering can be viewed as the "fundamental domains" constructed from representative group elements that in total correspond to the left and right coset spaces $SO(3)/\Gamma$ and $\Gamma \backslash SO(3)$.

In this paper, the shape of Voronoi cells for the tetrahedral group, the octahedral group, and the icosahedral group are studied. The discrete subgroup with the smallest Voronoi cells should be used for the sampling to minimize the distortion; a small-sized cell centered on the identity will be good for almost-uniform sampling because near the identity, $\exp \hat{\mathbf{x}} \approx \mathbb{I} + \hat{\mathbf{x}}$, and with $\mathbf{x}$ sampled uniformly in Cartesian coordinates, exponentiation does not warp the resulting rotations very much. Since the icosahedral group I has the largest number of group elements, $SO(3)$ is divided into smallest Voronoi cells compared to other discrete subgroups. Thus, to achieve best sampling results, the icosahedral group is used to generate the Voronoi cells in $SO(3)$. Fig. 2 shows that the center Voronoi cell shifted by a rotation matrix in the icosahedral group is overlapped with the Voronoi cell that corresponds to this rotation matrix. The Voronoi cells are visualized in the exponential coordinates.
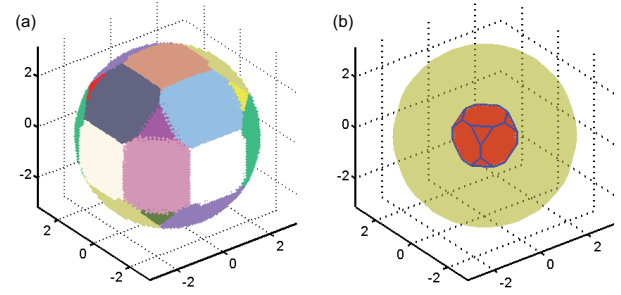

Fig. 1. (a) Voronoi cells of the octahedral group in $SO(3)$ are represented in exponential coordinates. Each color represents a Voronoi cell in $SO(3)$. We note that because the exterior Voronoi cells cover the interior ones in the figure, the regions with different colors may appear to be patches on a sphere but actually represent for sites in a solid ball. (b) The center Voronoi cell that corresponds to the identity matrix is represented in exponential coordinates. The yellow-shaded ball represents the solid ball in $\mathbb{R}^3$ with radius π.

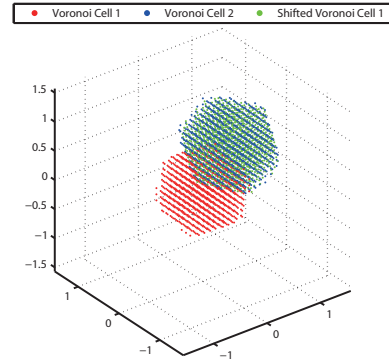
Fig. 2. The center Voronoi cell shifted by a rotation matrix R in the icosahedral group VS the Voronoi cell that corresponds to R. The complete overlapping between the two sites shows that the contents of the Voronoi cell on R can be replicated by the contents of the Voronoi cell on the identity by shifting the contents by R.

The shape of the Voronoi cells centered on the identity for the tetrahedral, octahedral and icosahedral groups are close to being polyhedra themselves; more specifically, they are almost cropped octahedron, cropped cube and dodecahedron [28]. We say "almost polyhedra" because the boundaries between the central cell and its neighbors are slightly curved inward, making the cell slightly rounded. But by considering the polyhedra that enclose the actual Voronoi cells, we can be guaranteed to cover $SO(3)$ with samples without gaps. And redundant points can easily be removed.

For the tetrahedral group, the center Voronoi cell is an octahedron cropped by surfaces normal to the axes through opposite vertices, with the distance $h_{C_2} = \pi/2$ from the origin (see Fig. 3 (a)). The Cartesian coordinates of the vertices on the cropped octahedron are

$$(\pm\sqrt{3}h_{C_3} \mp (\sqrt{3}h_{C_3} - h_{C_2}), \pm(\sqrt{3}h_{C_3} - h_{C_2}), 0), \quad (7)$$
$$(\pm\sqrt{3}h_{C_3} \mp (\sqrt{3}h_{C_3} - h_{C_2}), 0, \pm(\sqrt{3}h_{C_3} - h_{C_2})),$$
$$(\pm(\sqrt{3}h_{C_3} - h_{C_2}), \pm\sqrt{3}h_{C_3} \mp (\sqrt{3}h_{C_3} - h_{C_2}), 0),$$
$$(0, \pm\sqrt{3}h_{C_3} \mp (\sqrt{3}h_{C_3} - h_{C_2}), \pm(\sqrt{3}h_{C_3} - h_{C_2})),$$
$$(\pm(\sqrt{3}h_{C_3} - h_{C_2}), 0, \pm\sqrt{3}h_{C_3} \mp (\sqrt{3}h_{C_3} - h_{C_2})),$$
$$(0, \pm(\sqrt{3}h_{C_3} - h_{C_2}), \pm\sqrt{3}h_{C_3} \mp (\sqrt{3}h_{C_3} - h_{C_2})).$$

For the octahedral group, the center Voronoi cell is a cube with the center-to-face distance $h_{C4} = \pi/4$, cropped at each corner by a surface of a distance $h_{C_3} = \pi/3$ from the origin (see Fig. 3 (b)). The Cartesian coordinates of the vertices on the cropped cube are

$$h_{C_4}(\pm 1 \mp t, \pm 1, \pm 1) \tag{8}$$
$$h_{C_4}(\pm 1, \pm 1, \pm 1 \mp t)$$
$$h_{C_4}(\pm 1, \pm 1 \mp t, \pm 1),$$

where $t = 3\pi/4 - \sqrt{3}h_{C_3}$.

For the icosahedral group, the center Voronoi cell is a dodecahedron with the center-to-face distance $h_{C_5} = \pi/5$ (see Fig. 3 (c)). The Cartesian coordinates of the vertices on the dodecahedron are

$$c(\pm 1, \pm 1, \pm 1), \tag{9}$$
$$c(0, \pm 1/\varphi, \pm \varphi),$$
$$c(\pm 1/\varphi, \pm \varphi, 0),$$
$$c(\pm \varphi, 0, \pm 1/\varphi),$$

where $c = 20h_{C_5}/(\sqrt{250 + 110\sqrt{5}}(\sqrt{5} - 1))$.

D. Curvature of Cell Boundaries

Here we consider the shape of the boundary between the cell S_0 and and adjacent cell S_k centered on $\gamma_k = \exp(\theta_k \hat{\mathbf{n}}_k)$. This boundary is defined by the set of all $\mathbf{x} \in \mathbb{R}^3$ defined by the condition

$$d(\mathbb{I}, \exp(\hat{\mathbf{x}})) = d(\exp(\hat{\mathbf{x}}), \gamma_k). \tag{10}$$

When $\theta_k < 1$, this condition can be approximated by $\|\mathbf{x}\| = \|\mathbf{x} - \theta_k \mathbf{n}_k\|$, which defines a plane passing through $(\theta_k/2)\mathbf{n}_k$ with normal in the direction of $\mathbf{n}_k$. However, when θ_k is not small, (10) describes a surface with potentially significant curvature. This surface curves inward toward the origin from the plane described above, with which it shares the single point $\mathbf{x} = (\theta_k/2)\mathbf{n}_k$. This surface is a surface of revolution with axis $\mathbf{n}_k$. This can be seen from (10) and the bi-invariance of the metric, which implies invariance under conjugation (similarity transformations) as well. In particular, applying a similarity transformation to each entry in (10) with respect to $Q(\phi) = \exp(\phi \hat{\mathbf{n}}_k)$ where ϕ is an arbitrary angle of rotation gives

$$d(\mathbb{I}, \exp(\widehat{Q(\phi)\mathbf{x}})) = d(\exp(\widehat{Q(\phi)\mathbf{x}}), \gamma_k)$$

because $(Q(\phi)\hat{\mathbf{x}}Q^T(\phi))^\vee = Q(\phi)\mathbf{x}$ and $Q(\phi)\gamma_k Q^T(\phi) = \gamma_k$. Since these boundaries curve in, polyhedral descriptions of the cells are conservative, in that they contain all sample points in S_k, and can be depleted appropriately so as to avoid redundancy in sampling.

E. Distortion of Sampling

In this section, we calculate the distortion of our proposed sampling method and compare it with a widely used approach, the sampling based on Euler angles parametrization. Both methods are evaluated as (11),

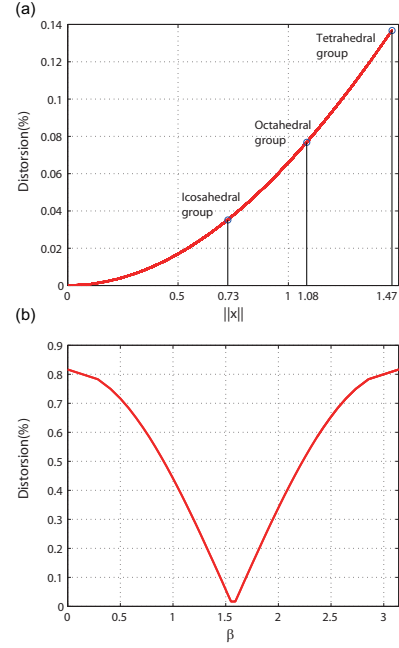$$C(\mathbf{q}) = \frac{1}{\sqrt{3}}\|G(\mathbf{q}) - \mathbb{I}\|, \tag{11}$$

Fig. 4. The distortion of the samples on $SO(3)$ using (a) our sampling method and (b) ZXZ Euler angles. In our sampling method, all the three discrete subgroups are evaluated on the norm of the Cartesian coordinates under exponential parameterization, $\|\mathbf{x}\|$. The maximum distortion for each discrete subgroup is marked in the figure. The icosahedron group should be used since it has the smallest Voronoi cell and results in the smallest distortion. By using the ZXZ Euler angles, the two Z rotations α and γ are sampled uniformly and the middle Euler angle β is sampled based on $\beta = \cos^{-1}(t)$, where t is sampled uniformly. In this case, the distortion is evaluated on each value of β from 0 to π.

The Jacobians for the $SO(3)$ exponential parameterization $R(\mathbf{x}) = \exp(\hat{\mathbf{x}})$ are known [29], [30]

$$J_l(\mathbf{x}) = \mathbb{I} + \frac{1 - \cos\|\mathbf{x}\|}{\|\mathbf{x}\|^2}X + \frac{\|\mathbf{x}\| - \sin\|\mathbf{x}\|}{\|\mathbf{x}\|^3}X^2, \tag{12}$$
$$J_r(\mathbf{x}) = \mathbb{I} - \frac{1 - \cos\|\mathbf{x}\|}{\|\mathbf{x}\|^2}X + \frac{\|\mathbf{x}\| - \sin\|\mathbf{x}\|}{\|\mathbf{x}\|^3}X^2,$$

where $\mathbf{x}$ is the Cartesian coordinates in exponential coordinates for $SO(3)$. Note that

$$J_l(\mathbf{x}) = J_r^T(\mathbf{x}) \quad \text{and} \quad J_l(\mathbf{x}) = R(\mathbf{x})J_r(\mathbf{x})$$

and $G(\mathbf{x}) = J_r^T(\mathbf{x})J_r(\mathbf{x}) = J_l^T(\mathbf{x})J_l(\mathbf{x})$. It can be shown that for $\|\mathbf{x}\| < \pi$ that

$$C(\mathbf{x}) \approx \frac{1}{12}\sqrt{\frac{2}{3}}\left(\|\mathbf{x}\|^2 - (\frac{\|\mathbf{x}\|}{3})^3\right). \tag{13}$$

In our sampling approach, the distortion by using the icosahedral group is shown in Fig. 4 (a). We can see that since the exponential parameterization is almost flat near the identity, when $\|\mathbf{x}\| \leq 0.1$, the distortion is almost zero. As $\|\mathbf{x}\|$ increases, the distortion becomes larger. But even at the furthest point of the center Voronoi cell, $\|\mathbf{x}\| = 0.73$, the distortion is only 3.52%. Since shifting the center Voronoi cell by rotational symmetry operation introduces no more distortion, it is the largest sampling distortion on $SO(3)$ and independent of the resolution of the Cartesian grids.
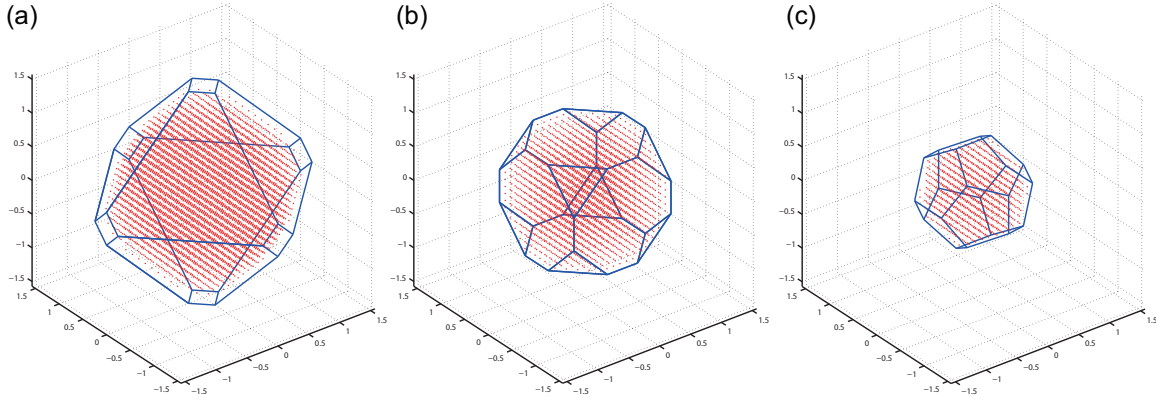
Fig. 3. The wire frame plots and an example of uniform Cartesian grids on the center Voronoi cells for the (a) tetrahedral, (b) octahedral and (c) icosahedral group. The plots are visualized in exponential coordinates.

Using the same measure, we also evaluate the distortion for ZXZ Euler angles (see Fig. 4 (b)). The Jacobians for the ZXZ Euler angles are [30]

$$J_l(\alpha,\beta) = \begin{pmatrix} 0 & \cos\alpha & \sin\alpha\sin\beta \\ 0 & \sin\alpha & -\cos\alpha\sin(\beta) \\ 1 & 0 & \cos\beta \end{pmatrix}, \quad (14)$$

$$J_r(\beta,\gamma) = \begin{pmatrix} \sin\beta\sin\gamma & \cos\gamma & 0 \\ \sin\beta\cos\gamma & -\sin\gamma & 0 \\ \cos\beta & 0 & 1 \end{pmatrix}.$$

The two Z rotations α and γ are sampled uniformly and the middle Euler angle β is sampled based on $\beta = \cos^{-1}(t)$, where t is sampled uniformly. The distortion remains the same using either the left or the right Jacobian. By using the sampling method based on Euler angles, even if the equal volume partitions of $SO(3)$ are achieved, we can see that the distortion is significantly large. As the value of β close to the singularity, i.e., $\beta = \pi$, the distortion increases and reaches the peak value 81.65%.

III. IMPLEMENTATION TO PROTEIN CRYSTAL PACKING PROBLEM

In applications ranging from robot motion planning to computational structure biology, generating a good set of samples is very important, particularly in the operations such as optimization, conformation searching, and path generation. A good set of sampling can substantially improve their computational speed and performance.

In this paper, we apply our sampling method to the problem of computing collision-free arrangements of articulated models of macromolecules packed in a crystal. This is important because crystallography is the main method used for obtaining structural and conformational information in the biomolecular sciences. Molecular replacement (MR) is a computational method that seeks to place a homologous/similar molecule in the crystallographic unit cell and search in the whole configuration space so as to maximize the correlation with x-ray diffraction data. See [28], [31] and references therein for a complete description of the MR method, including our approach, which involves the enumeration of all collision-free conformations.

In this "protein packing" problem, both collision checking and stochastic searching are involved, and their performance heavily relies on the sampling quality in the conformation space. To evaluate our sampling method, we look into a simplified toy model (similar to the one used in [31]) that simulates the packing of protein crystals. The rabbit-shaped toy model has fixed position and can rotate freely in space, in other words, the motion of the toy model is in $SO(3)$. The copies of the model tile the space in P1 symmetry, in which the copies retain the same motion (translation and rotation) with their positions shifted by the unit cell (see Fig. 5). Our goal is to obtain a sufficient candidate set of collision-free packing arrangements by using as few conformation searches as possible. We generate a similar number of samples on $SO(3)$ using both our proposed method and ZXZ Euler angles. In Fig. 6, we can see that when the number of samples is small (≤ 500), using Euler angles, no collision-free conformation is found while 42 are found using our sampling method. Even as the number of samples increases, we can always find more collision-free conformations using our method than sampling by Euler angles. The efficiency in finding collision-free candidates using our sampling method comes from the fact that the samples we generate in $SO(3)$ are more evenly spaced and have less distortion. Besides this protein crystal packing problem, our sampling method also have great potential in robot motion planning problem, which involves finding feasible conformations in high dimensional space.

IV. CONCLUSIONS

A new sampling method for the rotation group $SO(3)$ is proposed. In this method, $SO(3)$ is partitioned into Voronoi cells based on the rotational symmetry operations of the Platonic solids. Uniform Cartesian grids in exponential coordinates are generated on the Voronoi cell centered on the identity, and samples on the surrounding Voronoi cells are then replicated by shifting by the rotational symmetry operations. The shape of the Voronoi cells centered on the identity for the tetrahedral, octahedral and icosahedral groups are close to being polyhedra themselves. For the icosahedral group, the one has the smallest Voronoi cells, the largest
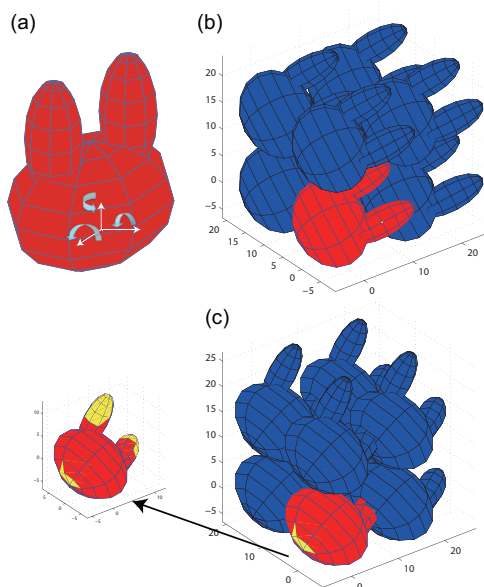
Fig. 5. (a) Illustration of 3 degrees of freedom in the packing model. Examples of packing configurations (b) without collisions (c) with collisions (indicated in yellow) [31].
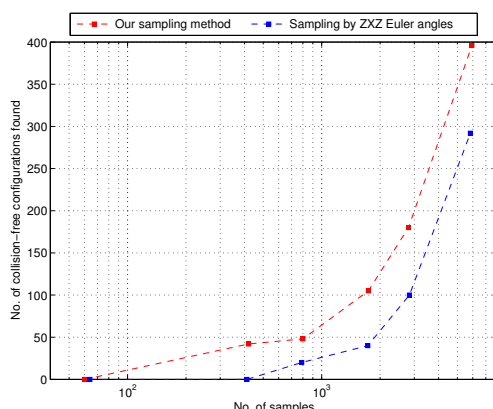

Fig. 6. The number of collision-free conformations VS the number of sample points on $SO(3)$ generated by (a) our sampling method, (b) sampling of Euler angles.

distortion is only 3.52%, independent of resolution of the Cartesian grid. This sampling method can achieve almost-uniform sampling at any level of resolution, without having to store large numbers of coordinates or requiring sophisticated data structures. In the implementation to protein crystal packing problem, the sampling method shows efficiency in finding collision-free conformations, and it can also apply to robot motion planning problem with great potential.

V. ACKNOWLEDGMENTS

REFERENCES

[1] Avro, J., "Fast Random Rotation Matrices," *Graphics Gems III* (D. Kirk, ed.), pp. 117-120, Academic Press, 1992.
[2] Chirikjian, G.S., *Stochastic Models, Information Theory, and Lie Groups, Vol. 2*, Birkhäuser, New York, Dec. 2011.
[3] Shoemake, K., "Uniform Random Rotations," *Graphics Gems III* (D. Kirk, ed.), pp. 124-132, Academic Press, 1992.
[4] E. Bannai, R. Damerell, Tight spherical designs, I , J. Math. Soc. Japan 31 (1979) 199-207.
[5] J.H. Conway, N.J.A. Sloane, Sphere packings, lattices and groups, third edition, Springer (New York) 1999.
[6] P. Delsarte, J.-M. Goethals, J.J. Seidel, Spherical codes and designs, Geometriae Dedicata 6 (1977) 363-388.
[7] Neutsch, W., Coordinates, de Gruyter, Berlin, 1996.
[8] B. W. Clare and D. L. Kepert, The optimal packing of circles on a sphere, J. Math. Chem., vol. 6, no. 4, pp. 325-349, May 1991.
[9] L. Fejes-Toth, Stable packing of circles on the sphere, Structural Topology, no. 11, pp. 9-14, 1985.
[10] D. A. Kottwitz, The densest packing of equal circles on a sphere, Acta Crystallogr. A, vol. 47, pt. 3, pp. 158-165, May 1991.
[11] T. Tarrnai, Spherical circle-packing in nature, practice and theory, Structural Topology, no. 9, pp. 39-58, 1984.
[12] S.L. Sobolev, Cubature formulas on the sphere which are invariant under transformations of finite rotation groups, Dokl. Akad. Nauk SSSR 146 (1962), 310-313.
[13] S.L. Sobolev, V.L. Vaskevich, The theory of cubature formulas, translated from the 1996 Russian original and with a foreword by S.S. Kutateladze, Kluwer Academic Publishers Group (Dordrecht) 1997.
[14] G. Yang, I. Chen, Equivolumetric partition of solid spheres with applications to orientation workspace analysis of robot manipulators, IEEE Transactions on Robotics, vol. 22, issue 5, pp. 869-879, 2006.
[15] E. E. Lattman, Optimal sampling of the rotation function, Acta Cryst B, vol. 28, issue 4, pp. 1065-1068, 1972.
[16] D. P. Hardin and E. B. Saff and D. P. Hardin and E. B. Saff, Discretizing manifolds via minimum energy points, Notices of the AMS, pp. 1186-1194, 2004.
[17] E. B. Saff and A. B. J. Kuijlaars, Distributing many points on a sphere, The mathematical Intelligencer, vol. 19, no. 1, pp. 5-11, 1997.
[18] K. M. Gorski and E. Hivon and A. J. Banday and B. D. Wandelt and F. K. Hansen and M. Reinecke and M. Bartelmann, HEALPix: A Framework for high-resolution discretization and fast analysis of data distributed on the sphere, The Astrophysical Journal, vol. 622, no. 2, pp. 759, 2005.
[19] S. R. Lindemann, A. Yershova and S. M. LaValle, Incremental grid sampling strategies in robotics, Algorithmic Foundation of Robotics VI, Springer Tracts in Advanced Robotics, Vol 17, 313-328, 2005.
[20] J. J. Kuffner, Effective sampling and distance metrics for 3D rigid body path planning, Proceedings of the 2006 IEEE ICRA, 2004.
[21] J. C. Mitchell, Sampling rotation groups by successive orthogonal images, SIAM J. Sci. Comput., vol. 30, issue 1, 525-547, 2008.
[22] X. Sun, Z. Chen, Spherical basis functions and uniform distribution of points on spheres, Journal of Approximation Theory, vol. 515, issue 2, 2008.
[23] G. Wagner, On a new method for constructing good point sets on spheres, Discrete and Computational Geometry, vol. 9, no. 1, pp. 111-129, 1993.
[24] A. Yershova, S. M. Lavalle, Deterministic sampling methods for spheres and $SO(3)$, Proceedings of the 2004 IEEE ICRA, 2004.
[25] A. Yershova, S. Jain, S. M. LaValle and J. C. Mitchell, Generating uniform incremental grids on $SO(3)$ using the Hopf Fibration, The International Journal of Robotics Research 2010 29: 801.
[26] G. S. Chirikjian and S. Zhou, Metrics on motion and deformation of solid models, ASME J. Mech. Des., vol. 120, no. 2, pp. 252-261, June 1998.
[27] Murray, R.M., Li, Z., Sastry, S.S., A Mathematical Introduction to Robotic Manipulation, CRC Press, Boca Raton, 1994.
[28] Chirikjian, G. S., Yan, Y., Mathematical aspects of molecular replacement. II. Geometry of motion spaces, Acta Crystallogr. A, vol. 68, issue 2, 2012.
[29] Park, F.C., The Optimal Kinematic Design of Mechanisms, Ph.D. Thesis, Division of Engineering and Applied Sciences, Harvard University, Cambridge, MA 1991.
[30] G.S. Chirikjian, A.B. Kyatkin, Engineering Applications of Noncommutative Harmonic Analysis, CRC Press, 2001.
[31] Y. Yan and G. S. Chirikjian, Molecular replacement for multi-domain structures using packing models, Proceedings of the ASME 2011 IDETC, 2011.